Phase Noise Performance of Optoelectronic Oscillators Based on Whispering-Gallery Mode Resonators

Romain Modeste Nguimdo, Khaldoun Saleh, Aurélien Coillet, Guoping Lin, Romain Martinenghi, and Yanne K. Chembo, *Senior Member, IEEE*

***Abstract*— Optoelectronic oscillators based on whispering-gallery mode resonators (WGMRs) are efficient oscillators for ultra-stable microwave generation, in which the energy can be stored in an ultra-high Q-factor resonator instead of the usual long delay line. In this paper, we derive a stochastic model for the calculation of the phase noise performance in these systems considering three different configurations, namely, the case where the energy is stored in high-Q disk-shaped WGMR, the case where energy is stored in an optical delay-line only, and the case for which the energy is stored simultaneously by the resonator and the delay line. Our investigations explain how the WGMR can be optimally used for spurious peak rejection in optoelectronic oscillators. Our experimental measurements are found to be in excellent agreement with analytical and simulation results.**

***Index Terms*— Optoelectronic oscillators, microwave generation, phase noise, whispering-gallery mode resonators.**

I. Introduction

ULTRA-PURE sinusoidal oscillations with frequency between 0.3 and 300 GHz are highly desired for several technological applications such as in radar, time-frequency metrology, lightwave technology, frequency synthesis, detection, and navigation systems. Typically, such signals can be generated by the so-called optoelectronic oscillators [1] (also referred to as OEOs), which have been initially proposed by Yao and Maleki [2]–[4]. In order to achieve ultra-high purity, OEOs generally use long fiber-delay lines (about 4 km of fiber length) inserted into the feedback loop in order to store the energy in the optical domain. However, this large optical delay introduces strong spurious ring-cavity peaks. The spectral purity of OEOs can be improved using techniques such as dual-loop configurations [5]–[9], or injection locking [10], [11] in order to suppress the spurious ring-cavity peaks. All these configurations are suitable for ultra-pure microwave generation, but however, the long fiber-based OEOs are typically bulky due to the weight and temperature-stabilized box containing the delay line. As a consequence, these systems are not easily transportable and cannot be easily miniaturized.

An alternative way to get around the above-mentioned drawbacks has consisted in replacing, in the OEO loop, the fiber delay-line by a whispering-gallery mode resonator (WGMR) with ultra-high Q-factor [12]–[14]. The insertion of a WGMR in the OEO loop also can provide an elegant solution for the realization of wideband tunable OEOs [15]. Whispering gallery mode resonators are low-loss dielectric disks which perform optical energy storage through trapping photons in the long-lifetime WGMR cavity. In this way, microwave oscillation is obtained by extracting the intermodal frequency of an optically pumped WGMR. From a technological point of view, the total photon lifetime in WGMRs can be as large as several tens of microseconds, and lead to a Q-factor as high as 10^{11} [16]. A theoretical model (supported by experiments) to describe WGMR-based OEOs has been recently proposed to investigate its deterministic dynamics [14]. Unlike usual OEOs without resonator [17]–[20], it is demonstrated that in the absence of the delay-line, the output of the microwave is unconditionally stable in the technologically achievable range of the loop gain. Despite these interesting features, it should be noticed that the most challenging task in OEOs lies on their phase noise performance which is indeed directly connected to their purity. A careful study of phase noise in WGMR-based OEOs is therefore an important step towards the optimization of this microwave generation system [21].

In this article, we derive a stochastic model for the study of phase noise performance in optoelectronic oscillators based on WGMRs, and perform experimental measurements to verify its validity. Contrary to ref. [15] where, for a structurally similar system, a WGMR is used only to select the optical mode

Manuscript received June 11, 2015; revised September 16, 2015; accepted October 1, 2015. Date of publication October 8, 2015; date of current version October 19, 2015. The work of R. M. Nguimdo was supported in part by Fonds National de la Recherche Scientifique, in part by the Research Foundation Flanders for project support and fellowships, and in part by the Belgian Interuniversity Attraction Pole Network photonics@be. The work of Y. K. Chembo was supported in part by the European Research Council through the StG NextPhase Project and PoC Versyt Project, in part by the Centre National d'Etudes Spatiales through the SHYRO Project, in part by the Région de Franche-Comté through the CORPS Project, and in part by the Labex ACTION. *(Corresponding author: Romain Modeste Nguimdo.)*

R. M. Nguimdo is with Optique Non Linéaire Théorique, Université Libre de Bruxelles, Brussels 1050, Belgium, and also with the Applied Physics Research Group, Vrije Universiteit Brussel, Brussels 1050, Belgium (e-mail: romain.nguimdo@vub.ac.be).

K. Saleh, G. Lin, R. Martinenghi, and Y. K. Chembo are with the Département d'Optique, FEMTO-ST Institute, Besançon 25030, France (e-mail: khaldoun.saleh@femto-st.fr; guoping.lin@femto-st.fr; romain.martinenghi@femto-st.fr; yanne.chembo@femto-st.fr).

A. Coillet is with NIST, Boulder, CO 80305 USA (e-mail: acoillet@gmail.com).

Color versions of one or more of the figures in this paper are available online at http://ieeexplore.ieee.org.

Digital Object Identifier 10.1109/JQE.2015.2488981

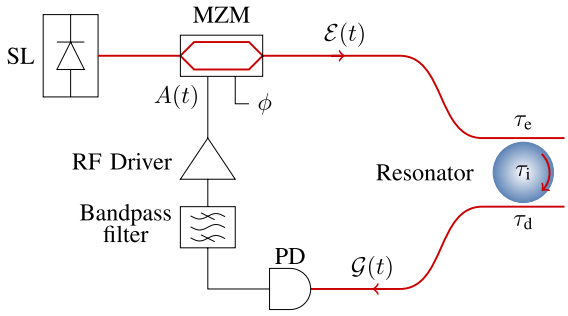

Fig. 1. Experimental setup as used in [14]. SL: continuous-wave semiconductor laser, MZM: Mach-Zehnder modulator, PD: photodiode. The optical path is in red, while the electric path is in black.

(resonator in add coupling only), we use a WGMR in add-drop coupling in order to select the optical mode meanwhile reducing/suppressing the spurious modes introduced by the delay-line. We also use a different theoretical approach to provide comprehensive investigation on the phase noise performance of such OEOs. More concretely, we consider both stochastic models for OEOs with and without delay line (DL) in the microwave loop. We also perform experiments that are compared with the theoretical results. The article is structured as follows. In Sec. II, we describe the system under study. The focus of Sec. III is the WGMR-based OEO model without delay-line, and its phase noise performance is analytically and numerically investigated. In Sec. IV, we study the model where a long delay line is combined with a WGMR in the feedback loop. In Sec. V, we compare the results of WGMR-based OEOs and usual DL-based OEOs without resonator, while Sec. VI is devoted to experimental measurements. Final remarks are given in Sec. VII.

II. The System

The architecture of the WGMR-based OEO under study is shown in Fig.1. It is an experimental setup recently introduced in refs. [14], [21] and it has the following single-loop structure. A laser beam with constant power P_0 is generated by a continuous-wave semiconductor laser. It is then injected into a Mach-Zehnder modulator (MZM) that is polarized and modulated by the electrical voltages V_B and $V(t)$, which are its bias and radio-frequency (RF) input voltages, respectively. These electrical signals modulate the optical light beam so that the envelope of the electric field at the MZM output reads

$$\mathcal{E}_{\mathrm{MZM}}(t) = \sqrt{P_0}\cos\left[\frac{\pi V(t)}{2V_{\pi\,\mathrm{RF}}} + \frac{\pi V_B}{2V_\pi}\right], \tag{1}$$

where $V_{\pi\,\mathrm{RF}}$ and V_π are the RF and DC half-wave voltages. This MZM output signal which has a broadband optical spectrum is coupled into a crystalline magnesium fluoride (MgF_2) WGMR through a tapered optical fiber. In this way, the intracavity field inside the resonator is excited by the field $\mathcal{E}_{\mathrm{MZM}}(t)$. Subsequently, the resonator output field is detected and fed to an RF filter with a central frequency Ω_0 and -3 dB bandwidth $\Delta\Omega$. The purpose of this bandpass filter is to reject the RF signal outside the frequency band of interest, and not to perform narrow-band filtering like in the conventional DL-based OEOs. Finally the signal at the output of the RF filter is amplified and applied to the RF electrode of the MZM in order to close the loop. Since the RF filter has a large bandwidth, the filtering process is achieved in the optical domain by the resonator only. Assuming that the WGMR output field is $\mathcal{G}(t)$, the RF filter output can be written as

$$V(t) = \eta G_0 P_0 S\,|\mathcal{G}(t)|^2, \tag{2}$$

where G_0 stands for the amplifier gain, η accounts for losses except in the WGMR, and S is the photodetection efficiency. By introducing a dimensionless voltage $x(t) = \pi V(t)/(2V_{\pi\,RF})$, the RF output voltage can be explicitly written as

$$x(t) = \beta\,|\mathcal{G}(t)|^2, \tag{3}$$

where $\beta = \pi\eta G_0 P_0 S/2V_{\pi\mathrm{RF}}$ is the optoelectronic gain when the effect of the WGMR is not accounted for. Note that an optical fiber can be inserted before or after the resonator in order to implement a delay in the microwave loop. We therefore consider the three following cases: (i) the case where the optical stability element is a resonator only (WGMR); (ii) the case where the optical stability element is an optical delay line only (DL); (iii) the case where the optical stability element is a combination of a WGMR and a DL serially connected (WGMR-DL). These three cases are referred to in the figures as WGMR, DL and WGMR-DL, respectively.

III. WGMR-Based OEOs Without Delay

A. Microwave Envelope

The WGMR is characterized by an intrinsic, an excitation (in-coupling) and a drop (out-coupling) photon lifetimes τ_i, τ_e and τ_d, respectively, and a free spectral range (FSR) Ω_M. These characteristics allow the WGMR to narrowly filter the input broadband optical spectrum $\mathcal{E}_{\mathrm{MZM}}(t)$ and deliver, at its output, a set of equidistant spectral lines separated by its FSR. Hence, the intracavity field $\mathcal{F}_R(t)$ of the WGMR is the sum of the optical spectral components $\mathcal{F}_R(t) = \sqrt{P_0}\sum_{-\infty}^{+\infty}\mathcal{F}_n e^{in\Omega_M t}$. In order to derive the equation governing the dynamics of each WGMR of interest, it is convenient to decompose $\mathcal{E}_{\mathrm{MZM}}(t)$ into its spectral components. Taking advantage of the fact that $x(t)$ can be expressed as $x(t) = A(t)\cos[\Omega_M t + \varphi(t)]$ for any microwave oscillator whose output angular frequency is around Ω_M, it can be straightforwardly demonstrated that [14]:

$$\mathcal{E}_{\mathrm{MZM}}(t) = \sqrt{P_0}\sum_{n=-\infty}^{n=+\infty}\mathcal{E}_n e^{in\Omega_M t}, \tag{4}$$

with

$$\mathcal{E}_n(t) = \epsilon_n(\phi)\mathrm{J}_n[A(t)]\,e^{in\varphi(t)}, \tag{5}$$

where J_n are the n^{th}-order Bessel functions of the first kind, with n being an integer; $\phi = \pi V_B/(2V_\pi)$ is the static phase of the MZM and $\epsilon_n(\phi) = \left[e^{i\phi} + (-1)^n e^{-i\phi}\right] i^n/2$. Therefore, each intracavity field component $\mathcal{F}_n(t)$ is excited by the corresponding $\mathcal{E}_n(t)$. This means that the WGMR intracavity

field is a multifrequency signal, and according to the Haus formalism, the dynamics of $\mathcal{F}_n(t)$ is ruled by [22]

$$\dot{\mathcal{F}}_n(t) = -\left[\frac{1}{\tau} + i\sigma\right]\mathcal{F}_n(t) + \sqrt{\frac{2}{\tau_e}}\mathcal{E}_n(t), \tag{6}$$

where $\sigma = \omega_L - \omega_0$ is the detuning frequency between the laser frequency ω_L and the central frequency of the pumped mode ω_0; $\tau^{-1} = \tau_i^{-1} + \tau_e^{-1} + \tau_d^{-1}$ corresponds to the inverse of the total lifetime of the photon in the resonator (this corresponds to the overall optical Q-factor $Q_{\text{opt-WGMR}} = \omega_L\tau$), when taking into account losses which arise from the coupling between the resonator and the optical fiber (see Fig. 1). The WGMR output signal is detected by a fast photodiode with a large bandwidth which rejects the frequencies above its cut-off frequency (the higher-order harmonics of the microwave signal are thereby rejected). In addition, its zero harmonic component is removed by the bandpass filter inserted after the photodiode. Since $\mathcal{G}(t) = \sqrt{2/\tau_d}\mathcal{F}_R(t)$, the right hand side of Eq. (3) therefore becomes

$$\begin{aligned}\beta\,|\mathcal{G}(t)|^2 &= \frac{2\beta}{\tau_d}\left|\sum_{n=-\infty}^{n=+\infty}\mathcal{F}_n e^{in\Omega_M t}\right|^2 \\ &\simeq 2\beta e^{i\upsilon}e^{i\Omega_M t}\sum_{n=-\infty}^{+\infty}\mathcal{G}_{n+1}\mathcal{G}_n^* + \text{c.c.}\end{aligned} \tag{7}$$

where υ represents the microwave round-trip phase shift and c.c. stands for the complex conjugate. Thus the deterministic features of the microwave envelope can be described in terms of the dimensionless slowly varying envelopes $\mathcal{G}_n(t)$ attached to the various modes, and the slowly varying envelope of the microwave $\mathcal{A}(t) = A(t)e^{i\varphi(t)}$ as [14]:

$$\dot{\mathcal{G}}_n = -\left[\frac{1}{\tau} + i\sigma\right]\mathcal{G}_n + \Gamma_n(\phi)\mathrm{J}_n\left[A(t)\right]e^{in\varphi(t)}, \tag{8}$$

$$\mathcal{A}(t) = 2\beta e^{i\upsilon}\sum_{n=-\infty}^{+\infty}\mathcal{G}_{n+1}\mathcal{G}_n^*, \tag{9}$$

with $\Gamma_n(\phi) = 2\epsilon_n(\phi)/\sqrt{\tau_d\tau_e}$.

In addition, the microwave is also subjected to noise originating from various sources (laser, resonator, photodiode, etc.). This noise indeed introduces fluctuations around the steady state solutions, and these stochastic phenomena can be modeled by including Langevin noise terms to the core deterministic model. Two main noise contributions can be considered. The first contribution is multiplicative noise, resulting from the overall optical gain fluctuations. It is composed from very different noise contributions, but for the sake of simplicity, it will be assumed in this study as Gaussian white noise with empirical noise power density $|\eta_n(\omega)|^2 = 2D_m$. The multiplicative noise can be taken into account in the model by multiplying the last term of Eq. (8) by $[1 + \eta_n(t)]$ where $\eta_n(t)$ is a dimensionless multiplicative noise. The second contribution is additive noise which is related to environmental fluctuations. For each spectral line, this noise is also considered as a complex-valued Gaussian white noise $\zeta_n(t)$ with zero mean-value and correlation $\langle\zeta_n(t)\zeta_n^*(t')\rangle = 2D_a\delta(t-t')$, corresponding to the density power spectrum $|\zeta_n(\omega)|^2 = 2D_a$. The signal at the output of the resonator experiences additional additive noise from the photodiode before being read out as the microwave signal is measured at the output of the RF filter (see Fig. 1).

Therefore, taking into account all noise terms, the stochastic model to describe the noisy slowly-varying envelope $\mathcal{A}(t)$ can be written as

$$\begin{aligned}\dot{\mathcal{G}}_n = &-\left[\frac{1}{\tau} + i\sigma\right]\mathcal{G}_n \\ &+ \Gamma_n(\phi)\Big[1 + \eta_n(t)\Big]\mathrm{J}_n\left(A\right)e^{in\varphi} + \sqrt{\frac{2}{\tau_d}}\zeta_n(t),\end{aligned} \tag{10}$$

$$\mathcal{A}(t) = 2\beta e^{i\upsilon}\sum_{n=-\infty}^{+\infty}\mathcal{G}_{n+1}\mathcal{G}_n^*. \tag{11}$$

From Eqs. (10) and (11), it can be seen that although all microwave harmonics are filtered out during the process, the complex amplitude and the noise generated in all the optical modes do affect the microwave.

B. Non-Trivial Fixed Point and Its Stability

For $\dot{\mathcal{G}}_n = 0$ and $\dot{\mathcal{A}} = 0$, there is a trivial fixed point $\mathcal{A}^{st} = 0$ which exists for every value of the loop gain. However, a non-trivial fixed point can also emerge for some values of this gain. If we consider $\mathcal{G}_n(t) = G_n(t)e^{i\Psi_n(t)}$ and $\mathcal{A}(t) = A(t)e^{i\varphi(t)}$, the non-trivial fixed point is defined by:

$$G_n^{st} = \frac{\tau\Gamma_n(\phi)}{\sqrt{\left(1+\sigma^2\tau^2\right)}}\mathrm{J}_n\left(A^{st}\right), \tag{12}$$

$$A^{st} = \Gamma\mathrm{J}_1\left(2A^{st}\right), \tag{13}$$

where

$$\Gamma = \frac{4\beta\tau^2|\sin(2\phi)|}{\tau_e\tau_d\left(1+\sigma^2\tau^2\right)} \tag{14}$$

is the overall gain (positive by convention) satisfying $\Gamma > 1$ [14]. This non-trivial fixed point is of great interest since it corresponds to the microwave amplitude. In ref. [14], it has been shown that the non-trivial fixed point satisfies $0 < A^{st} \leq 1.91$ for $\Gamma > 1$. Moreover, this fixed point is unconditionally stable for $1 < \Gamma < 15.52$ when there is no delay-line.

C. Phase Noise Performance

A convenient way to evaluate the purity of the microwave is to measure its phase noise spectrum. In the regime of stable microwave emission, the effects of noise on the amplitude are typically negligible meaning that such amplitude can be assumed as constant [i.e $A(t) \simeq A^{st}$ and $G_n(t) \simeq G_n^{st}$]. Thus the stochastic phase equations from Eqs. (10) and (11) can be written as

$$\begin{aligned}\dot{\Psi}_n = &-\sigma + \Gamma_n(\phi)\Big[1 + \eta_n(t)\Big]\frac{\mathrm{J}_n\left(A^{st}\right)}{G_n^{st}}\sin\left[n\varphi - \Psi_n\right] \\ &+ \sqrt{\frac{2}{\tau_d}}\frac{\zeta_{n,\Psi}(t)}{G_n^{st}},\end{aligned} \tag{15}$$

$$0 = \sum_{n=-\infty}^{+\infty}G_{n+1}^{st}G_n^{st}\sin\Big[\Psi_{n+1} - \Psi_n + \upsilon - \varphi\Big], \tag{16}$$

where $\zeta_{n,\Psi}(t) = \zeta_{n,Re}(t)\sin(-\Psi_n) + \zeta_{n,Im}(t)\cos(-\Psi_n)$ are independent Gaussian white noises with spectral density $|\tilde{\zeta}_{n,\Psi}(\omega)|^2 = 2D_a$ and $|\tilde{\zeta}_{n,\varphi}(\omega)|^2 = 2D_a$. The sub-indices Re and Im refer to the real and imaginary parts.

As noise corresponds to small fluctuations around the stable steady states, all higher-order terms can be disregarded. Thus, Eqs. (15) and (16) can be rewritten as

$$\dot{\Psi}_n = \Gamma_n(\phi)\frac{\mathrm{J}_n\left(A^{st}\right)}{G_n^{st}}\sin\left[n\varphi^{st} - \Psi_n^{st}\right]\eta_n(t) + \sqrt{\frac{2}{\tau_d}}\frac{\zeta_{n,\Psi}(t)}{G_n^{st}} + \Gamma_n(\phi)\frac{\mathrm{J}_n\left(A^{st}\right)}{G_n^{st}}\cos\left[n\varphi^{st} - \Psi_n^{st}\right]\Big[n\varphi - \Psi_n\Big], \quad (17)$$

$$0 = \sum_{n=-\infty}^{+\infty} G_{n+1}^{st}G_n^{st}\Big[\Psi_{n+1} - \Psi_n - \varphi\Big]. \quad (18)$$

By making use of the steady state solutions given in Eqs. (12) and (13), and assuming that $\sin x \simeq x$, one finally obtains

$$\dot{\Psi}_n = \sigma\,\eta_n(t) + \frac{1}{\tau}\Big[n\varphi - \Psi_n\Big] + \sqrt{\frac{2}{\tau_d}}\frac{\zeta_{n,\Psi}(t)}{G_n^{st}}, \quad (19)$$

$$0 = \sum_{n=-\infty}^{+\infty} G_{n+1}^{st}G_n^{st}\Big[\Psi_{n+1} - \Psi_n - \varphi\Big]. \quad (20)$$

Since Eqs. (19) is linear, the phase noise spectrum in the whole frequency range can be obtained from the squared modulus of its Fourier transform. Hence, considering that all noise sources are uncorrelated, the squared modulus of the Fourier transform of $\varphi(t)$ is

$$\Big|\Phi(\omega)\Big|^2 = \frac{2\sigma^2\alpha_1^2\Big|\eta(\omega)\Big|^2 + \dfrac{4D_a}{\tau_d}\alpha_2^2}{\omega^2}, \quad (21)$$

where the coefficients α_1^2 and α_2^2 are explicitly defined as

$$\alpha_1^2 = \frac{2\sum_{n=0}^{+\infty}\mathrm{J}_n^2\left(A^{st}\right)\mathrm{J}_{n+1}^2\left(A^{st}\right)}{\mathrm{J}_1^2\left(2A^{st}\right)}, \quad (22)$$

$$\alpha_2^2 = \frac{1}{\mathrm{J}_1^2\left(2A^{st}\right)\sin^2 2\phi}. \quad (23)$$

Equation (21) shows that the phase noise depends on the detuning between the laser and the resonator pumped mode. As another interesting remark, Eq. (21) also shows that the effect of the multiplicative noise can completely vanish provided that the laser frequency and the pumped mode are perfectly matched (i. e $\sigma = 0$). This is explained by the fact that this detuning is in fact an intensity-to-phase noise conversion mechanism. In practice, it is possible to match the two frequencies with great accuracy, even though thermal effects might induce additional detuning.

IV. WGMR-Based OEOs With Delay

A. Model

In a typical WGMR-based OEO, a delay time can result from the optical fiber connecting the different stand-alone components. This delay time is usually in the order of nanoseconds, which indeed has negligible effect on the dynamics and the purity of the microwave. However, as in usual OEOs without resonator, a long delay can be deliberately implemented using an optical fiber. Considering that such optical fiber is inserted between the MZM and the resonator, the signal coming out from the MZM is delayed in time before being coupled into the resonator. In this case, Eqs. (10) and (11) can be rewritten as

$$\dot{\mathcal{G}}_n = -\left[\frac{1}{\tau} + i\sigma\right]\mathcal{G}_n + \sqrt{\frac{2}{\tau_d}}\zeta_n(t) + \Gamma_n(\phi)\Big[1 + \eta_n(t)\Big]\mathrm{J}_n\left(A_T\right)e^{in(\varphi_T - \omega_L T)}, \quad (24)$$

$$\mathcal{A}(t) = 2\beta e^{i\upsilon}\sum_{n=-\infty}^{+\infty}\mathcal{G}_{n+1}\mathcal{G}_n^*, \quad (25)$$

where T is the delay time, $A_T \equiv A(t-T)$ and $\varphi_T \equiv \varphi(t-T)$. Note the appearance of $e^{-in\omega_L T}$ which is a static feedback phase originating from the optical path followed by each spectral component in the fiber. Without loss of generality, we set $e^{-in\omega_L T} = 1$ as it just shifts the microwave phase $\varphi(t)$. The fixed point solutions of Eqs. (24) and (25) are the same as those obtained for the system without delay.

B. Phase Noise Spectrum

Proceeding as in Sec. III-C, the phase noise derived from Eqs. (24) and (25) can be described in time domain by the following linear equations:

$$\dot{\Psi}_n = \sigma\,\eta_n(t) + \frac{1}{\tau}\Big[n\varphi_T - \Psi_n\Big] + \sqrt{\frac{2}{\tau_d}}\frac{\zeta_{n,\Psi}(t)}{G_n^{st}}, \quad (26)$$

$$0 = \sum_{n=-\infty}^{+\infty} G_{n+1}^{st}G_n^{st}\Big[\Psi_{n+1} - \Psi_n - \varphi\Big]. \quad (27)$$

In Fourier domain, the squared modulus of the Fourier transform of $\varphi(t)$ obtained from Eqs. (26) and (27) is

$$\Big|\Phi(\omega)\Big|^2 = \frac{2\sigma^2\alpha_1^2\Big|\eta(\omega)\Big|^2 + \dfrac{4D_a}{\tau_d}\alpha_2^2}{\left|i\omega + \dfrac{1}{\tau}\left(1 - e^{-i\omega T}\right)\right|^2}. \quad (28)$$

For $T = 0$, one recovers the phase noise spectrum formula given by Eq. (21). It is also seen that the WGMR linewidth defined as $\Delta\omega = 1/\tau$ can eventually play a role when $T \neq 0$.

For our forthcoming simulations, we consider the following experimental parameters [14], unless otherwise stated: $\tau_i = 6.5\ \mu$s, $\tau_e = 29\ \mu$s, $\tau_d = 1\ \mu$s. These parameters lead to an overall lifetime $\tau = 0.84\ \mu$s corresponding to $\Delta\omega \approx 1.2$ MHz and an optical Q-factor $Q_{\mathrm{opt-WGMR}} = \omega_L\tau = 1.02 \times 10^9$ for a laser operating at a frequency $f_L = 192$ THz (i.e $\lambda = 1552.2$ nm). This value of optical Q-factor corresponds to an RF Q-factor

$$Q_{\mathrm{RF-WGMR}} = Q_{\mathrm{opt-WGMR}} \times \frac{\Omega_0}{f_L} \approx 0.33 \times 10^5 \quad (29)$$

for $\Omega_0 \approx 6$ GHz. Note that the value of $\Delta\omega$ we are considering clearly ensures the filtering in the optical domain only as it is much smaller than $\Delta\Omega$ which is $\approx$10 MHz. Other parameters of interest are $\phi = -\pi/4$, $D_m = 10^{-8}$ rad^2/Hz,

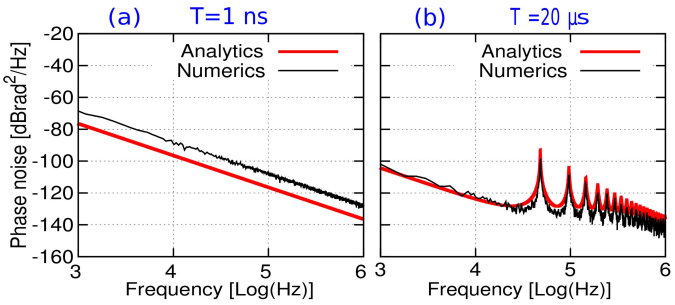

Fig. 2. Analytical and numerical phase noise spectra for (a) $T = 1$ ns and (b) $T = 20$ μs. $A^{st} = 0.56$.

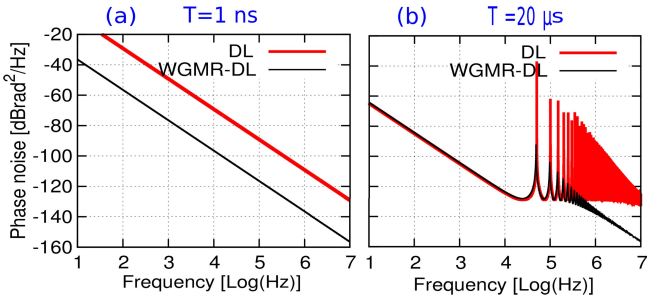

Fig. 3. Comparison between the phase noise performance of DL-based OEO with WGMR (black) and without a resonator (gray, red in color) for (a) $T = 1$ ns and (b) $T = 20$ μs. $A^{st} = 0.56$.

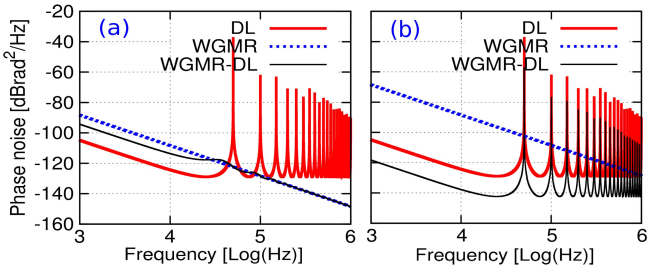

Fig. 4. Comparison between the phase noise performance of DL-based OEO with a WGMR and without a WGMR when (a) the delay-line and the WGMR have identical RF Q-factor ($Q_{\mathrm{RF-WGMR}} = Q_{\mathrm{RF-DL}} = 7.5 \times 10^5$) considering $\Delta\omega = 1.2$ MHz and $\Delta\Omega = 10$ MHz; (b) the RF filter and the WGMR have identical bandwidth ($\Delta\omega = \mu = 31.4$ MHz) $Q_{\mathrm{RF-DL}} = 7.5 \times 10^5$.

$D_a = 5 \times 10^{-8}$ rad^2/Hz, $\sigma/2\pi = 0.16$ kHz, $\beta = 24.16$ and $A^{st} = 0.56$.

For $T = 20$ μs (corresponding to 4 km of fiber length), the phase noise spectra obtained both analytically and numerically are shown in Fig. 2, and they can be compared with those obtained with a negligible delay ($T = 1$ ns). It is seen that both analytics and numerics predict a significant improvement of the phase noise performance for long delays. More precisely, both the analytical and numerical predictions show that the phase noise can be improved by approximately 25 dB. To provide a better understanding regarding the role of each optical stability element, we next compare the phase noise spectra of DL-based OEOs with and without resonator.

V. Comparison Between the Phase Noise Performance of DL-Based OEOs With and Without Resonator

For the usual DL-based OEOs without a resonator, a stochastic model to describe its dynamics has been proposed in [19]:

$$\dot{\mathcal{A}} + \mu e^{i\upsilon}\mathcal{A} = \gamma\, e^{i\upsilon}\,[1+\eta(t)]\,\mathrm{J}_1(2A_T)\,e^{i\varphi_T} + \mu e^{i\upsilon}\zeta_a, \qquad (30)$$

where $\gamma = \pi\eta G_0 P_0 S|\sin 2\phi|/2V_{\pi\mathrm{RF}}$ is the effective overall loop gain and $\upsilon = \arctan(1/2Q_f)$, with $Q_f \approx \Omega_0/\Delta\Omega$ being the quality factor provided by the RF filter of half-bandwidth $\mu/\pi \approx \Delta\Omega$ in the microwave branch. From Eq. (30), the theoretical phase noise spectrum has been derived as [19]:

$$|\Psi(\omega)|^2 = \frac{\dfrac{\mu^2}{4Q_f^2}|\eta(\omega)|^2 + \dfrac{2\mu^2}{|A^{st}|^2}D_a}{|i\omega + \mu(1-e^{-i\omega T})|^2}. \qquad (31)$$

Equation (31) is to be compared with Eq. (28). From the comparison with experiments, we consider $D_m = 10^{-8}$ rad^2/Hz, and $D_a = 3.0 \times 10^{-14}$ rad^2/Hz, $\Omega_0 = 6$ GHz and $\Delta\Omega = 10$ MHz. These parameters lead to $Q_f \simeq 600$ and $\mu/\pi = 10$ MHz. Figure 3 shows the results for phase noise performance in DL-based OEO without a resonator calculated from Eq. (31), and with a WGMR obtained from Eq. (28) for $T = 1$ ns and $T = 20$ μs. The RF Q-factor $Q_{\mathrm{RF-DL}}$ of these delay-lines is 37.6 and 7.5×10^5 respectively for a microwave frequency $\Omega_0 = 6$ GHz. For $T = 1$ ns (i.e short delay lines), it is seen that the phase noise in WGMR-based OEOs is ~38 dB better than that obtained in DL-based OEOs without a resonator. This is because the RF Q-factor generated by this delay length is much smaller than that of the WGMR (i.e $Q_{\mathrm{RF-WGMR}} \gg Q_{\mathrm{RF-DL}}$). Increasing the delay to $T = 20$ μs so that $Q_{\mathrm{RF-WGMR}} \ll Q_{\mathrm{RF-DL}}$ (i.e using long delay lines), the exactly same phase noise performance is obtained in both OEOs with and without a WGMR. This is because although the WGMR and the optical fiber individually provide a Q-factor each, their serial combination does not significantly improve the overall effective Q-factor to lead to an improvement in the phase noise with the chosen parameters. However, it is interesting to note that the WGMR allows to significantly reduce the spurious peaks. In particular the reduction for the first-neighboring spur is ≈55 dB.

Now we focus upon the case for which RF Q-factor of the delay-line and that of the WGMR are equal. More precisely, we increase $Q_{\mathrm{RF-WGMR}}$ to 7.5×10^5 (same as $Q_{\mathrm{RF-DL}}$) corresponding to $\tau = 19.1$ μs. This increase of $Q_{\mathrm{RF-WGMR}}$ implies the decrease of $\Delta\omega$ by a factor of 22.72 (i.e $\Delta\omega = 0.052$ MHz). The phase noise spectra are shown in Fig. 4(a) for WGMR-based OEOs with and without delay in comparison with the DL-based OEO without the resonator. In particular, the case for which a WGMR is combined with a delay line having the same Q-factor indicates that the spurious peaks are completely suppressed (black line). In addition, the phase noise performance is in-between that obtained individually with the OEO with a WGMR only (dashed line) and with fiber delay-line only (red line), when the frequency ω is smaller than $1/T$ although the Q-factor is twice larger in this case. The fact that the phase noise performance in this frequency range is worse than that obtained in the DL-based configuration without a WGMR is because the increase of the

Q-factor is accompanied with the decrease of the linewidth $\Delta\omega$ [see Eq. (28)].

To estimate the effects of the OEO bandwidth, we consider again $Q_{\mathrm{RF-DL}} = 7.5 \times 10^5$ and set the WGMR linewidth to be equal to the RF filter bandwidth, i.e $\Delta\omega = \mu = 31.4$ MHz. This increase of $\Delta\omega$ implies the decrease of $Q_{\mathrm{RF-WGMR}}$ by a factor of 26.41 (i.e $Q_{\mathrm{RF-WGMR}} = 0.012 \times 10^5$). Figure 4(b) shows the results for the different configurations. It turns out that the OEO with both the WGMR and the delay-line achieves a better performance than the OEO with the delay line only although the overall RF Q-factor is the same in both cases. This improvement is about 18 dB as compared to the case for which a 4 km long DL only is used as the stability element. However, it should be noticed that the spurious peaks become stronger, and even reach the same level as those obtained with a 4 km long DL only. This clearly evidences the role that the WGMR plays in reducing or suppressing the spurious peaks.

VI. Experimental Results

In order to confirm our theoretical results, we have performed experimental measurements considering different energy storage elements. We use a wideband integrated optics $LiNbO_3$ MZM with $V_{\pi\mathrm{RF}} = 4.7$ V, $V_\pi = 4$ V and $V_B = 2$ V seeded by an SL delivering a maximum optical power $P_0 = 30$ dBm. A polarization controller is also used to tune the polarization at the input of the WGMR. For WGMR-based configuration, the laser lightwave is coupled into and out of the WGMR by evanescent field through two tapered optical microfibers in an add-drop configuration. Our experimental setup is built using a 12 millimeters diameter MgF_2e disk-shaped WGMR (the 12 mm diameter is the raw disks diameter before the fabrication process, which consists in grinding and polishing). The laser wavelength is stabilized onto the optical mode of interest by using a low frequency Pound-Drever-Hall (PDH) laser stabilization loop (see ref. [21], [23] for details). This technique is optimized for laser-WGMR stabilization and specifically for a selected optical mode. The characterization of the WGMR in the optical domain has allowed us to retrieve the following parameter values: $\tau_i = 6.5$ μs, $\tau_e = 29$ μs, $\tau_d = 1$ μs (these values are used for theoretical estimations), FSR $\sim$ 6 GHz. For the usual delay-based configuration, a 4 km long single mode optical fiber has been used to connect the MZM output and a fast photodiode while for the combination of the both elements, the WGMR output was connected to the same photodiode using the same 4 km long single mode optical fiber. The long delay line was placed in a thermally isolated box where its temperature is uniformly and actively stabilized. The transmission losses η after the stabilization were measured to be 6 dB, 2.2 dB and 8.4 dB for OEO configurations with the WGMR only, with the delay line only, and with the combination of both, respectively. The optical signals were read by a fast photodiode with a conversion factor $S = 50\ \Omega \times 0.65$ A/W $= 32.5$ V/W, and bandwidth 0−12 GHz. Subsequently, the photodiode output signal crossed a narrow-band microwave RF filter of central frequency at 6.25 GHz and a bandwidth of 10 MHz in order to reject the RF noise outside

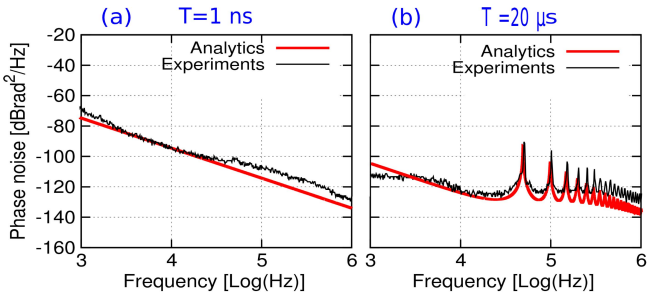

Fig. 5. Comparison between analytical and experimental phase noise spectra for (a) $T = 1$ ns and (b) $T = 20$ μs.

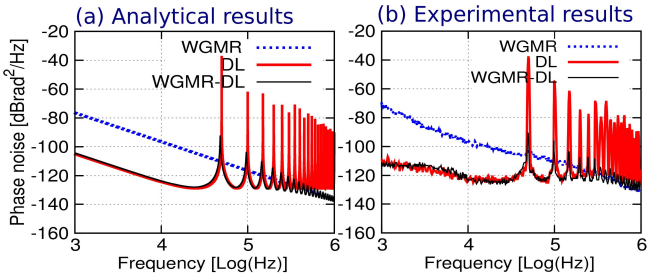

Fig. 6. (a) Analytical and (b) experimental estimations of phase noise spectra of the three OEOs based each on different optical stability elements: a MgF_2 WGMR (blue), a 4 km long DL (red), and a 4km long delay line combined with a MgF_2 WGMR (black).

the frequency band of interest. This leads to exactly the same Q-factors as used for theoretical estimations. The different measurements were accomplished using an APEX 2440B optical spectrum analyzer (OSA) and a Rohde & Schwarz FSW50 electrical signal and spectrum analyzer (ESSA). The peak-to-peak generated microwave amplitude is 3.34 V and its frequency is $\sim$6 GHz. Note that, for each configuration, the optical power seeding the MZM is set so as to have the same overall microwave loop gain (and therefore the same generated microwave amplitude).

For comparison we display in Fig. 5 the analytical and experimental phase noise spectra for OEO stabilized with a WGMR only (negligible delay length) [Fig. 5(a)] and when the WGMR is combined with a 4 km long delay line [Fig. 5(b)]. The experimental estimations of phase noise spectra are those of microwaves generated at $\sim$6 GHz. On the one hand, it is seen that the phase noise spectrum is as low as -67 dBrad^2/Hz and -127 dBrad^2/Hz at 1 kHz and 1 MHz, respectively when the noise in the OEO loop is rejected only by the MgF_2 WGMR. This result is in excellent agreement with analytical results shown in Fig. 5(a). When the same MgF_2 WGMR is serially connected to a 4 km long of an optical delay fiber, the experimental results indicate a phase noise performance of -107 dBrad^2/Hz and -124 dBrad^2/Hz at 1 kHz to 1 MHz, respectively (black). This is again in good agreement with analytical results which show a phase noise spectra of -104 dBrad^2/Hz and -125 dBrad^2/Hz in the same frequency range (red). This corresponds, in both cases, to an improvement of $\approx$25 dB as compared to the case for which the noise is rejected by the resonator only. In particular, Fig. 5(b) indicates an excellent agreement between the spurious peaks obtained with the model and those from experiments. For further insight, we now compare the phase noise spectra of

WGMR-based OEOs with those obtained in DL-based OEOs without resonator. Figure 6 shows the estimated (a) and the measured (b) phase noise spectra in a window from 1 kHz and 1 MHz considering the three OEO configurations, each based on a different optical stability element. A very similar phase noise performance is theoretically (a) and experimentally (b) obtained when the WGMR is removed (this corresponds to the case for which the OEO bandwidth is now defined by RF bandpass filter). As such the OEO configuration becomes that of usual DL-based OEO (i.e without the resonator). This confirms the analytical and numerical predictions that the serial combination of delay line and a WGMR with ultra-high Q-factor is an efficient method for spurious peak rejection, if the laser-WGMR add-drop light coupling configuration is well optimized.

Note that phase noise is often expressed in units of dBc/Hz. The relation between the two units for sideband phase noise is: [dBrad^2/Hz]=[dBc/Hz]+3dB.

VII. Conclusion

We have derived a stochastic model to describe the effects of noise on the microwave phase dynamics. Using these equations, we have analytically and numerically estimated the phase noise performance of WGMR-based OEOs with and without delay. In both cases, we have found that the spectral purity in these devices depends on the detuning between the laser frequency and the central frequency of the resonator pumped mode. Comparing the results for DL-based OEOs with and without a resonator, we have found that WGMR-based OEOs with DL display a strong rejection rate for spurious peaks, thereby leading to higher spectral purity. In particular when the WGMR and the delay-line have equal ultra-high Q-factor, the WGMR acts as a mode discriminator and is able to filter out completely the closely spaced OEO modes defined by the delay line. But the phase noise performance degrades close to the microwave frequency as compared with the case for which the same delay-line is used without the resonator. However, a better phase noise performance can be also obtained close to the microwave frequency when a WGMR with a larger linewidth is considered, but in return the spurious peaks become stronger. This suggests that a good compromise should be found between using a WGMR with a large linewidth and that with ultra-high Q-factor. Our different OEOs configurations have been experimentally tested and the experimental results showed an excellent agreement with theoretical (analytical and numerical) results thus evidencing the validity of our theoretical approach. Experimental results also have confirmed that a good compromise has to be found in order to obtain a high loaded Q and low insertion loss for the WGMR. This is directly linked to the laser-WGMR add-drop light coupling configuration that has to be very well optimized.

References

[1] L. Maleki, "The optoelectronic oscillator," *Nature Photon.*, vol. 5, no. 12, pp. 728–730, 2011.

[2] X. S. Yao and L. Maleki, "High frequency optical subcarrier generator," *Electron. Lett.*, vol. 30, no. 18, pp. 1525–1526, Sep. 1994.

[3] X. S. Yao and L. Maleki, "Optoelectronic microwave oscillator," *J. Opt. Soc. Amer. B*, vol. 13, no. 8, pp. 1725–1735, 1996.

[4] X. S. Yao and L. Maleki, "Optoelectronic oscillator for photonic systems," *IEEE J. Quantum Electron.*, vol. 32, no. 7, pp. 1141–1149, Jul. 1996.

[5] X. S. Yao, L. Maleki, Y. Ji, G. Lutes, and M. Tu, "Dual-loop opto-electronic oscillator," in *Proc. IEEE Int. Freq. Control Symp.*, May 1998, pp. 545–549.

[6] L. Maleki, S. Yao, Y. Ji, and V. Ilchenko, "New schemes for improved opto-electronic oscillator," in *Proc. Int. Topical Meeting Microw. Photon.*, vol. 1. 1999, pp. 177–180.

[7] D. Eliyahu and L. Maleki, "Low phase noise and spurious level in multi-loop opto-electronic oscillators," in *Proc. IEEE Int. Freq. Control Symp. PDA Exhibit. Jointly 17th Eur. Freq. Time Forum*, May 2003, pp. 405–410.

[8] J. Yang, Y. Jin-Long, W. Yao-Tian, Z. Li-Tai, and Y. En-Ze, "An optical domain combined dual-loop optoelectronic oscillator," *IEEE Photon. Technol. Lett.*, vol. 19, no. 11, pp. 807–809, Jun. 1, 2007.

[9] R. M. Nguimdo, Y. K. Chembo, P. Colet, and L. Larger, "On the phase noise performance of nonlinear double-loop optoelectronic microwave oscillators," *IEEE J. Quantum Electron.*, vol. 48, no. 11, pp. 1415–1423, Nov. 2012.

[10] E. C. Levy, O. Okusaga, M. Horowitz, C. R. Menyuk, W. Zhou, and G. M. Carter, "Comprehensive computational model of single- and dual-loop optoelectronic oscillators with experimental verification," *Opt. Exp.*, vol. 18, no. 20, pp. 21461–21476, 2010.

[11] O. Okusaga *et al.*, "Spurious mode reduction in dual injection-locked optoelectronic oscillators," *Opt. Exp.*, vol. 19, no. 7, pp. 5839–5854, 2011.

[12] K. Volyanskiy, P. Salzenstein, H. Tavernier, M. Pogurmirskiy, Y. K. Chembo, and L. Larger, "Compact optoelectronic microwave oscillators using ultra-high Q whispering gallery mode disk-resonators and phase modulation," *Opt. Exp.*, vol. 18, no. 21, pp. 22358–22363, 2010.

[13] A. B. Matsko, L. Maleki, A. A. Savchenkov, and V. S. Ilchenko, "Whispering gallery mode based optoelectronic microwave oscillator," *J. Modern Opt.*, vol. 50, nos. 15–17, pp. 2523–2542, 2003.

[14] A. Coillet, R. Henriet, P. Salzenstein, K. P. Huy, L. Larger, and Y. K. Chembo, "Time-domain dynamics and stability analysis of optoelectronic oscillators based on whispering-gallery mode resonators," *IEEE J. Sel. Topics Quantum Electron.*, vol. 19, no. 5, Sep./Oct. 2013, Art. ID 6000112.

[15] D. Eliyahu *et al.*, "Resonant widely tunable opto-electronic oscillator," *IEEE Photon. Technol. Lett.*, vol. 25, no. 15, pp. 1535–1538, Aug. 1, 2013.

[16] A. A. Savchenkov, A. B. Matsko, V. S. Ilchenko, and L. Maleki, "Optical resonators with ten million finesse," *Opt. Exp.*, vol. 15, no. 11, pp. 6768–6773, 2007.

[17] Y. K. Chembo, L. Larger, H. Tavernier, R. Bendoula, E. Rubiola, and P. Colet, "Dynamic instabilities of microwaves generated with optoelectronic oscillators," *Opt. Lett.*, vol. 32, no. 17, pp. 2571–2573, 2007.

[18] Y. K. Chembo, L. Larger, and P. Colet, "Nonlinear dynamics and spectral stability of optoelectronic microwave oscillators," *IEEE J. Quantum Electron.*, vol. 44, no. 9, pp. 858–866, Sep. 2008.

[19] Y. K. Chembo, K. Volyanskiy, L. Larger, E. Rubiola, and P. Colet, "Determination of phase noise spectra in optoelectronic microwave oscillators: A Langevin approach," *IEEE J. Quantum Electron.*, vol. 45, no. 2, pp. 178–186, Feb. 2009.

[20] Y. K. Chembo, A. Hmima, P.-A. Lacourt, L. Larger, and J. M. Dudley, "Generation of ultralow jitter optical pulses using optoelectronic oscillators with time-lens soliton-assisted compression," *J. Lightw. Technol.*, vol. 27, no. 22, pp. 5160–5167, Nov. 15, 2009.

[21] K. Saleh *et al.*, "Phase noise performance comparison between opto-electronic oscillators based on optical delay lines and whispering gallery mode resonators," *Opt. Exp.*, vol. 22, no. 26, pp. 32158–32173, 2014.

[22] H. A. Haus, *Waves and Fields in Optoelectronics*. Englewood Cliffs, NJ, USA: Prentice-Hall, 1984.

[23] E. D. Black, "An introduction to Pound–Drever–Hall laser frequency stabilization," *Amer. J. Phys.*, vol. 69, no. 1, pp. 79–87, 2001.

Romain Modeste Nguimdo received the M.Sc. degree in theoretical physics with a minor in option mechanics from the University of Dschang, Dschang, Cameroon, and the University of Yaoundé I, Yaoundé, Cameroon, in 2006, and the M.Sc. degree in theoretical physics and the Ph.D. degree from the Instituto de Fsica Interdisciplinar y Sistemas Complejos, Palma de Mallorca, Spain, in 2008 and 2011, respectively. From 2012 to 2015, he was a Post-Doctoral Fellow with the Applied Physics Research Group, Vrije Universiteit Brussel, Brussels, Belgium. He is currently an Fonds National de la Recherche Scientifique Fellow with the Université Libre de Bruxelles, Brussels. His current research interests include nonlinear dynamics, optical chaos cryptography, and ultrapure microwaves, random bit generation, and delay-based reservoir computing.

Khaldoun Saleh received the Ph.D. degree in microwaves, electromagnetism, and optoelectronics from Toulouse III University, France, in 2012. He is currently with the Franche-Comté Electronique, Mécanique, Thermique et Optique–Sciences et Technologies Institute, Besanon, France, as a Research Engineer. His research interests involve microwaves, optoelectronics, microwave-photonics, and nonlinear optics, and are particularly focused on the development of ultrastable optical and microwave reference sources based on ultrahigh-Q and ultrastable optical cavities.

Aurélien Coillet received the Ph.D. degree from the University of Burgundy, Dijon, France, in 2011. From 2012 to 2014, he was a Post-Doctoral Fellow with the Franche-Comté Electronique, Mécanique, Thermique et Optique–Sciences et Technologies Institute, Besanon, France, and is currently with the National Institute of Standards and Technology, Boulder, CO, USA. His research interests include ultra high-Q whispering gallery mode resonators, optoelectronics, nonlinear optics, and nonlinear dynamics.

Guoping Lin received the Ph.D. degree in optics from Xiamen University, China, and the Ph.D. degree in physics from École Normale Supérieure, Paris, France, in 2010. From 2011 to 2013, he was a National Aeronautics and Space Administration Post-Doctoral Program Fellow with the Jet Propulsion Laboratory, Pasadena, USA. He is currently a Post-Doctoral Fellow with the Franche-Comté Electronique, Mécanique, Thermique et Optique–Sciences et Technologies Institute, Besanon, France, where he is working on miniature spectrally pure microwave sources based on ultra high-Q crystalline optical resonators.

Romain Martinenghi received the Ph.D. degree in photonic reservoir computing from the Franche-Comté Electronique, Mécanique, Thermique et Optique–Sciences et Technologies (FEMTO-ST) Institute, Besanon, France, in 2012. He is currently with the FEMTO-ST Institute as a Post-Doctoral Research Fellow on the stabilization of high spectral purity microwave sources.

Yanne K. Chembo (SM'12) received the Ph.D. degree in physics from the University of Yaoundé I, in 2005, and the Ph.D. degree in laser physics from the Institute for Cross-Disciplinary Physics and Complex Systems, Palma de Mallorca, Spain, in 2006. In 2007 and 2008, he was a Post-Doctoral Fellow with the Franche-Comté Electronique, Mécanique, Thermique et Optique–Sciences et Technologies (FEMTO-ST) Institute, Besanon, France. In 2009, he was a National Aeronautics and Space Administration Post-Doctoral Program Fellow with the Jet Propulsion Laboratory, Pasadena, USA. Since 2010, he has been a Senior Research Scientist with the Centre National de la Recherche Scientifique, with affiliation with the FEMTO-ST Institute. He has authored over 100 articles in international journals and conference proceedings. His research interests involve microwave photonics, optoelectronics, complex systems, and applied nonlinear, stochastic, and quantum dynamics.